Satellite Image Compression by Post-Transforms in the Wavelet Domain

X. Delaunay [a,*], M. Chabert [b], V. Charvillat [b], G. Morin [b]

[a] *CNES/TéSA/NOVELTIS, Parc Technologique du Canal, 31520 Ramonville-Saint-Agne, France*

[b] *IRIT/ENSEEIHT, 2 rue C. Camichel, 31071 Toulouse Cedex 7, France*

Abstract

This paper proposes a novel compression scheme with a tunable complexity-rate-distortion trade-off. As images increase in size and resolution, more efficient compression schemes with low complexity are required on-board Earth observation satellites. The standard of the Consultative Committee for Space Data Systems (CCSDS) defines a strip-based compression scheme with the advantages of a low complexity and an easy rate control [1]. However, future mission specifications expect higher performance in terms of rate-distortion. The scheme proposed in this paper intends to perform better than the CCSDS standard while preserving low complexity and easy rate control. Moreover, to comply with existing on-board devices, the proposed core compression engine still uses the wavelet transform but in association with a linear post-processing inspired from the bandelet transform. The post-transform decomposes a small block of wavelet coefficients on a particular basis. This basis is adaptively selected within a predefined dictionary by rate-distortion optimization. The computational complexity depends upon the dictionary size and of the basis structure. An extremely simple dictionary, reduced to the Hadamard basis, is proposed. The post-transform efficiency is illustrated by experiments on various Earth

observation images provided by the French Space Agency (CNES).

Key words: Still image coding, Discrete transforms, Wavelet transform, Satellite application

---

1 Introduction

The decorrelation process is an important step in a classical compression scheme based on transform coding. Indeed, images are highly spatially correlated. Thus, if no decorrelation was applied, many pixels should be jointly encoded to obtain a bit-rate close to the minimal entropy. However, high dimension vector coding requires huge computational capabilities and is thus impracticable on-board. Appropriate transforms allow to decorrelate the data and to reduce low order entropies. The transformed coefficients can thus be quantized and then encoded nearly independently by a low complexity entropy coder [2]. Currently, the best state-of-the-art compression results have been obtained with the discrete wavelet transform (DWT). This paper proposes to associate the DWT with an appropriate post-transform to improve the decorrelation step with a tunable complexity increase.

Despite fair properties, the DWT presents some limitations. First, many bits are required to encode strong DWT coefficients associated to edges and textures. Second, dependencies remain between local neighboring DWT coefficients [3–5]. Future on-board image compression techniques should overcome these limitations. Currently, the remaining dependencies are exploited

* Corresponding author.
Email address: xavier.delaunay@noveltis.fr (X. Delaunay).

by smartly designed encoders. Coders from the zero-tree family [6,7] exploit inter- and intra-band redundancies by using a tree-like encoding of the positions of large zero areas in the bit-planes. The Bit-Plane Encoder (BPE) of the CCSDS [1] recommendation [1] which specially targets on-board compression may be classified into this family. The Embedded Block Coding with Optimal Truncation Points (EBCOT) algorithm of JPEG2000 standard [8,9] uses contextual bit-plane coding. A clever adaptive scan of the bit-planes exploits intra-band redundancies along geometrical structures such as edges. Finally, morphological coders [10,11] build clusters of significant coefficients and apply region growing techniques to exploit the redundancy associated to image structures. The storage of the significant bit lists requires a high memory capacity. Moreover, the implementation is difficult since the adaptive scan of the coefficients depends on significant bits.

Another way to go beyond the limitations of the DWT is to design more powerful transforms. Since 2000, many new transforms have been proposed in the literature to compete with the DWT [12–14]. Many, such as the curvelets [12], introduce directionality and anisotropy in the basis elements and are successful in restoration tasks. Unfortunately, few preserve the critical sampling feature, and the resulting redundancy is a huge penalty for compression. The bandelet transform [14] is an orthogonal non-redundant post-transform. This article applies to on-board compression and generalizes the bandelet transform: the proposed compression method derives from the bandelet transform and is called the post-transform compression scheme in the following. As the ban-

[1] The CCSDS is an international consortium including the major space agencies in the world such as the European Spatial Agency (ESA), the National Aeronautics and Space Administration (NASA) and the CNES (Centre National d'Etudes Spatiales).

delet transform by groupings proposed by Peyré in [14,15], the post-transform applies on the DWT coefficients. First a 2-dimensional DWT of the image is derived using the wavelet recommended by the CCSDS. Second, small blocks of DWT coefficients are linearly transformed by projection on an optimal basis selected in a predefined dictionary by rate-distortion optimization. Because it applies on small blocks, this process is not memory demanding and could be implemented on hardware for strip-based on-board compression. Moreover, this very simple processing only performs vectorial dot products. Finally, the dictionary size can be adapted to computational capacities.

The proposed post-transform is compared to the original bandelet transform in terms of compression results and complexity for various dictionaries. In particular, low complexity solutions are investigated for on-board implementation purpose. Indeed, the post-transform compression scheme has adjustable computational complexity. Moreover, this scheme parameters (block size, rate-distortion criterion and dictionary composition) has been optimized on a learning set of 12-bit high resolution satellite images provided by the French Space Agency (CNES). Finally, the proposed compression scheme is compared to the CCSDS and JPEG2000 standards in terms of rate-distortion. Note however that, according to the CCSDS recommendation, JPEG2000 is too complex for on-board compression [16]. The CCSDS recommendation provides many arguments against the use of JPEG2000 in this context: JPEG2000 may be parallelized but requires three coding passes for each bit-plane. Second, the optimal JPEG2000 rate control has high implementation complexity whereas the sub-optimal rate control is inaccurate [16]. In [17], some contexts in the EBCOT coder have been removed in order to reduce JPEG2000 complexity. Although a good compression performance was maintained, the complexity

	SPOT4 (1998)	SPOT5 (2002)	PLEIADES (2010)
Swath	60 km	60 km	20 km
Resolution	10 m	2.5 m	0.7 m
Bit-rate	32 Mb/s	128 Mb/s	4.5 Gb/s

Table 1
Resolutions and bit-rates of French Earth observation satellites.

gain was not sufficient.

The paper is organized as follows: section 2 presents the needs and constraints for on-board spacecraft compression. Section 3 introduces the general principles of the post-transform for compression. Section 4 proposes different post-transform dictionaries. Section 5 studies the associated compression performance obtained with these bases. Section 6 concludes the paper.

2 On-board compression: needs and constraints

Table 1 gives the data rates at the input of the compression system of three recent French Earth observation missions: SPOT4, SPOT5 and PLEIADES. This table illustrates the increasing on-board compression needs. The main on-board constraints are strip-based input format produced by push-broom acquisition mode, limited down-link capacity and limited on-board computational capacity. First, as the satellite travels Earth surface up and down, the optical sensors produce an image of fixed width but with a virtually endless length. Therefore, this image has to be compressed and transmitted during its acquisition. For this reason, images will be processed by blocks of 16 lines

(a) PLEIADES image (b) DWT of the image

Fig. 1. (a) PLEIADES panchromatic simulated image and the associated DWT.

on the future PLEIADES satellites. Second, even when the satellite is visible from a receiver station on-ground, the down-link rate is limited. Hence, a buffer is generally used on-board to store the data that cannot be transmitted in real time. Nevertheless, the buffer capacity remains limited. Consequently, the output bit-rate of the compressor must be controlled. Coders that produce embedded bit-streams such as the BPE of the CCSDS [1] are thus recommended. Bit-rate regulation is then possible by simple truncation of the bit-stream whatever the bit-rate. On the contrary, as mentioned in the introduction, a reliable tuning of JPEG2000 bit rate has a high computational cost [16]. Indeed, JPEG2000 encoder imposes specific truncation points.

On the SPOT5 satellite launched in 2002, the decorrelator is the Discrete Cosine Transform (DCT) [18]. On PLEIADES satellites, the decorrelator will be the DWT. Figure 1 displays a simulated PLEIADES panchromatic image with a resolution of 70 cm and the associated DWT. The PLEIADES compression scheme associates the DWT to a low complexity bit-plane coder which produces an embedded bit-stream. A challenging issue for future on-board

compressor is to exploit or to reduce the remaining dependencies between DWT coefficients to improve compression performance. The proposed post-transform compression scheme is intended to reduce these dependencies while maintaining a low complexity.

3 Post-transform in the wavelet domain

The DWT of the images is performed on three levels of decomposition using the lossy 9/7 biorthogonal float filters recommended by the CCSDS [1]. In order to exploit remaining redundancies between DWT coefficients, blocks of coefficients in all subbands, except the low-frequency subband (LL_3), are further transformed independently. No blocking artifacts are visible on the reconstructed image since the blocks are processed in the wavelet domain. First, the choice of an appropriate block size must be discussed.

3.1 Remaining redundancies

Joint-probabilities between DWT coefficients have been modeled in [4]. In [3], mutual information measurements between two or more DWT coefficients have shown that most dependency is intra-band. The proposed post-transform precisely aims at exploiting intra-band redundancies. Table 2 displays the estimated statistical dependencies in terms of correlation coefficient r and mutual information I_r between pairs of DWT coefficients as a function of their distance. The estimation has been performed from 7 satellite images i.e. on more than 7.2 millions of DWT coefficients. The distance d between pairs of coefficients is 1, 2 or 3 pixels in vertical or horizontal direction. High pass direc-

	Distance d	1	2	3
High pass direction	Correlation coefficient r	-0.54	0.13	-0.01
	Mutual information I_r	15.3%	4.4%	2.8%
Low pass direction	Correlation coefficient r	0.18	-0.01	0.01
	Mutual information I_r	8.4%	4.8%	3.8%

Table 2

Statistical dependencies between pairs of wavelet coefficients.

tion denotes pairs of coefficients horizontally (respectively vertically) aligned in the subband HL_1 (respectively LH_1). Low pass direction denotes pairs of coefficients vertically (respectively horizontally) aligned in the subband HL_1 (respectively LH_1). The relative mutual information I_r is defined by:

$$I_r(X,Y) = \frac{2\,(H_0(Y) - H_0(Y|X))}{H_0(X) + H_0(Y)} \tag{1}$$

where $H_0(X)$ is the zero order entropy of X. $I_r(X,Y)$ can be interpreted as the proportion of information that can be saved to encode Y if X is already known. For entropy derivation, the quantization operation must be taken into account. A quantization step q lead to a particular bit-rate after arithmetic coding. For I_r computation in table 2, the quantization step has been set to $q = 32$. This value leads to a bit-rate near 2 bpp targeted for on-board compression of 12-bit Earth observation images. Table 2 emphasizes that, in the DWT of 12-bit high resolution satellite Earth observation images, intra-band redundancies between DWT coefficients is confined to a small neighborhood. Thus, the post-transform is applied to small blocks. For an on-board satellite compression application, processing small blocks is less memory intensive and requires less computational capabilities. Moreover, since the blocks are

processed independently, the process can be parallelized to achieve real-time compression. Finally such processing is suitable for a strip-based input format as produced by push-broom type sensors. Indeed, the compression can begin whereas the image acquisition is not completed. In the following, DWT coefficients are processed by blocks of size 4×4. This block size is a good compromise for the compression: the bigger the blocks, the more complex the computation. However when the block size decreases, the number of blocks and thus the side information increases as explained in the following.

3.2 Post transform general principle

For each block of 4×4 DWT coefficients, the best post-transform decomposition basis is chosen among a dictionary of bases by minimization of a rate-distortion criterion. This method leads to compression performance improvement in terms of rate-distortion with respect to the DWT alone. Indeed, the canonical basis, which corresponds to the absence of post-transform, belongs to the dictionary. However, there are two main drawbacks: the need to signal to the decoder which post-transform basis has been chosen on each block and the computational cost of the basis selection. Indeed , the selected basis identifier, or so-called side information in the following, must be sent for each block. Moreover, although only one basis is retained for each block, the decomposition on all the bases in competition must be computed to select the best one. Robert *et al.* have designed a similar process in [19] to enhance the compression performance of the video coder H.264. Blocks of size 4×4 are circularly shifted according to nine different orientations before DCT derivation. The best orientation is selected by optimization of a rate-distortion criterion.

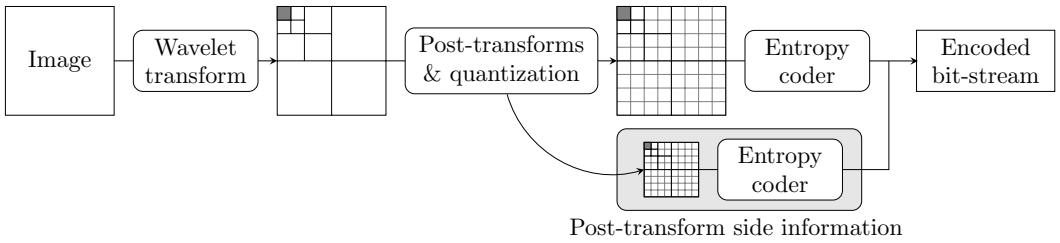

Fig. 2. Post-transform compression scheme.

The optimization requires the derivation of the nine possible shifts and their associated DCT on each block. The selected shift must be transmitted. Unfortunately, the slight decorrelation improvement is compensated by the bit-rate increase due to shift signaling. On the contrary, the post-transform proposed in this paper globally enhances the compression performance.

The post-transform compression scheme is outlined on figure 2. Blocks of DWT coefficients of all the subbands except the LL_3 (low-pass) subband are post-transformed and quantized. The compressed bit-stream is composed of the entropy coded post-transform coefficients and side information. The entropy coder is the adaptive arithmetic coder provided in [20].

The post-transform of one block is detailed on figure 3. Each block of DWT coefficients denoted by f is linearly transformed in order to obtain a representation f^{b*} more effectively compressible. The linear post-transforms are defined in a dictionary $\mathcal{D}$ known by both the encoder and the decoder. This dictionary contains $N_{\mathcal{B}}$ different orthonormal bases. Let $\mathcal{B}_b = \{\phi_m^b\}_{m=1}^M$ denote the basis number b with $b \in \{1, \ldots, N_{\mathcal{B}}\}$. The ϕ_m^b are the associated basis vectors and $M = 16$ is the space dimension. Blocks can be viewed as vectors of $\mathbb{R}^{16}$. The post-transformed representation f^b of f simply results from a change of basis, from the canonical basis to one of the bases of the dictionary $\mathcal{D}$:

$$f^b = \sum_{m=1}^{M} < f, \phi_m^b > \phi_m^b.$$

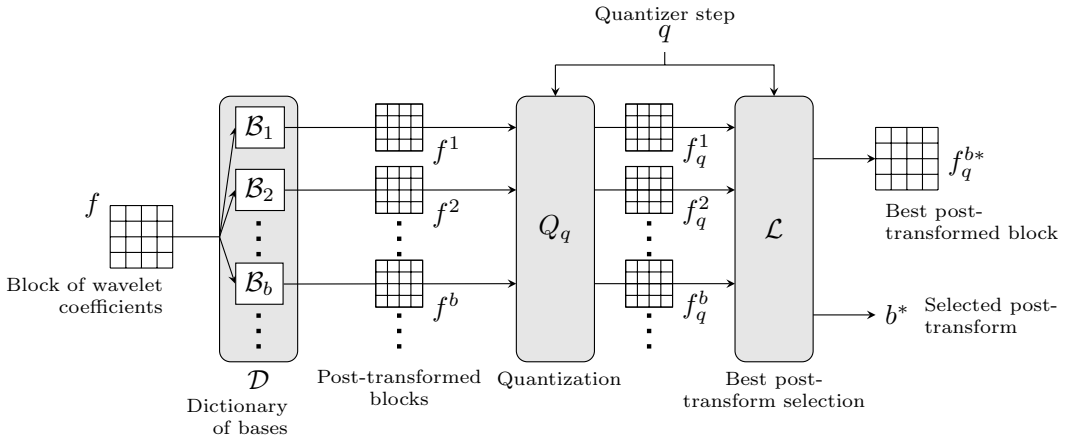

Fig. 3. Post-transform of one block of wavelet coefficients.

The quantized representations are denoted by f_q^b where q is the quantization step of the uniform scalar quantizer with double dead-zone Q_q:

$$Q_q(x) = \begin{cases} 0 & \text{if } |x| < q \\ \text{sign}(x)(k+1/2)\,q & \text{if } kq \leq |x| < (k+1)\,q. \end{cases}$$

This is the commonly used quantizer for DWT compression. It has been shown theoretically and numerically in [21] that it is close to the best choice to minimize the distortion. On each block, f_q^{b*} denotes the best representation in terms of compression among all the quantized representations f_q^b, $b \in \{1, \ldots, N_{\mathcal{B}}\}$.

The post-transform coding algorithm is summarized in figure 4. The different steps of the algorithm as well as the chosen parameters are discussed in the following. The decoding process is very simple. The post-transformed coefficients f_q^{b*} are first inversely quantized. The DWT coefficients can be reconstructed using the side information on each block. Finally, the inverse DWT gives the reconstructed image.

Input: An image
Output: The compressed bit-stream

Wavelet transform the image;
Quantization and encoding of the LL subband;

foreach *subband of the wavelet transform except the LL subband* **do**
    Compute the histogram of the subband to evaluate
    the probabilities $\Pr(Q_q(a[m]))$;
    Split the subband into 4×4 blocks;
    foreach *block* f **do**
        foreach *basis* $\mathcal{B}_b$ *of the dictionary* $\mathcal{D}$ **do**
            Post-transform the block f in the basis $\mathcal{B}_b$;
            Quantize f^b using the quantizer Q_q;
            Evaluate the cost $\mathcal{L}(f_q^b)$;
        end
        Keep the representation f_q^{b*} which minimizes
        the rate-distortion criterion $\mathcal{L}(f_q^b)$;
        Keep the identifier b^* of the basis used to obtain that
        representation;
    end
    Encode the basis identifiers of the selected representations
    for each block of that subband using an entropy coder;
    Encode the quantized post-transformed coefficients
    using an entropy coder;
end

Fig. 4. Post-transform compression algorithm.

3.3 Rate distortion trade-off

The best representation f_q^{b*} of each block is selected using a rate-distortion criterion after quantization of the representations f^b, $b \in \{1, \ldots, N_{\mathcal{B}}\}$.

Lagrangian criterion The rate-distortion trade-off can be adjusted using the Lagrangian $\mathcal{L}(f_q^b)$ defined by:

$$\mathcal{L}(f_q^b) = D(f_q^b) + \lambda\, R(f_q^b) \tag{2}$$

where the distortion $D(f_q^b)$ is a measure of the square error due to the quantization and $R(f_q^b)$ is an estimation of the bit-rate needed to encode the post-transformed block and the side information. Finally, λ is the Lagrangian mul-

tiplier optimized for the compression. The distortion is computed by:

$$D(f_q^b) = \|f^b - f_q^b\|^2 = \sum_{m=1}^{M} |a_b[m] - Q_q(a_b[m])|^2$$

where the $a_b[m]$, $m \in \{1, \ldots, M\}$ are the coefficients of the representation f^b. Since the post-transform is orthonormal, the square error can be computed in the transform domain.

Bit-rate estimation The bit-rate can be expressed by $R(f_q^b) = R_c(f_q^b) + R_b$, where $R_c(f_q^b)$ is the bit-rate allocated to the quantized representation f_q^b and R_b is the bit-rate allocated to the side information. The first term $R_c(f_q^b)$ is estimated by the entropy of the quantized post-transformed coefficients:

$$R_c(f_q^b) = -\sum_{m=1}^{M} \log_2 \Pr\left(Q_q(a_b[m])\right).$$

The probabilities $\Pr\left(Q_q(a_b[m])\right)$ of the post-transformed coefficients cannot be directly estimated at this stage since they depend on the selection of the best representation of each block. Therefore, these probabilities are estimated from the histogram of each DWT subband. However, for a given quantization step, the observed kurtosis (respectively entropy) is higher (respectively lower) after the post-transform. Indeed, the kurtosis (respectively entropy) measures how peaky (respectively smooth) is the probability distribution of a random variable. For example, on the HL_1 subbands of the image displayed on figure 1, the kurtosis of the post-transform is 41.9 and the kurtosis of the DWT is 27.2. According to tables 3 and 4, the entropy of the DWT $H_0(W)$ is 1.675 bpp and the entropy of the post-transform $H_0(PT)$ is 1.584 bpp for the same image and quantization step $q = 32$. Nevertheless, the total bit-rate of the post-transform $R(PT) + R(\text{side information})$ is increased up to 1.794 bpp because of the side information. This bit-rate increase is balanced by a quality increase according

Entropy $H_0(W)$	Bit-rate $R(W)$	PSNR(W)
1.675 bpp	1.714 bpp	50.04 dB
1.746 bpp	1.794 bpp	50.48 dB

Table 3

Rate-distortion trade-off for image 1(a) with the quantized wavelet coefficients W and an adaptive arithmetic coder.

$\hat{H}_0(PT)$	$H_0(PT)$	$R(PT)$	$R(PT) + R$(side information)	PSNR(PT)
1.589 bpp	1.584 bpp	1.627 bpp	1.794 bpp	51.17 dB

Table 4

Rate-distortion trade-off for image1(a) with the quantized post-transformed coefficient PT and an adaptive arithmetic coder.

to the PSNR comparison in tables 3 and 4. Table 4 shows that the entropy of the post-transform coefficients estimated from the DWT histogram $\hat{H}_0(PT)$ is very close to the true entropy $H_0(PT)$. Moreover, the true bit-rate $R(PT)$ obtained with the adaptive arithmetic coder is well estimated by $\hat{H}_0(PT)$ with a relative error of only 2.4%. Finally, several tests on large satellite images lead to the same observation. Note that table 3 and 4 are not intended to compare the DWT and post-transform compression performance. They rather aim at illustrating the sharing out between rate and distortion for the post-transform. The DWT is used as a reference. Compression performance will be compared in section 5.

The second term R_b is computed by:

$$R_b = -\log_2 \Pr(b) \quad \text{with} \quad \Pr(b) = \begin{cases} 0.5 & \text{if } b = 0 \\ 0.5/N_{\mathcal{B}} & \text{if } b \in \{1, ..., N_{\mathcal{B}}\}. \end{cases}$$

The post-transform denoted by $b = 0$ is the identity, that is, the block of DWT coefficients is not post-transformed. In most blocks, DWT coefficient decorrelation is sufficient for an efficient compression. Therefore, to favor this "non transformation", the prior probability $\Pr(0)$ is fixed to a higher value than the other probabilities $\Pr(b)$ for $b \in \{1, \ldots, N_{\mathcal{B}}\}$. This reduces the rate-distortion cost $\mathcal{L}(f_q^0)$ compared to the other costs $\mathcal{L}(f_q^b)$.

Lagrangian multiplier In [22], Le Pennec gives a theoretical expression of the optimal Lagrangian multiplier: $\lambda = \frac{3}{4\gamma_0}\, q^2$ with $\gamma_0 = 6.5$. This expression is based on a low bit-rate assumption. γ_0 is the ratio between the total bit-rate and the number of non-zero quantized coefficients. This ratio has been found approximately constant at low and medium bit-rates in [21]. This optimal Lagrangian multiplier jointly minimizes the rate and the distortion for the quantization step q. Another value of λ would give a higher distortion with the same bit-rate or higher bit-rate with the same distortion, for this quantization step. In [23], we have derived a similar expression under the high bit-rate assumption: $\lambda = \frac{\ln(2)}{6}\, q^2$. This assumption may hold at bit-rate greater than 2 bpp targeted for on-board compression. The numerical value of this expression is very close to the previous one: $\lambda \approx 0.115\, q^2$. However, an optimization process, similar to the Shoham and Gersho approach [24], performed on several Earth observation images, has shown that $\lambda \approx 0.15\, q^2$ leads to a slight performance improvement [23].

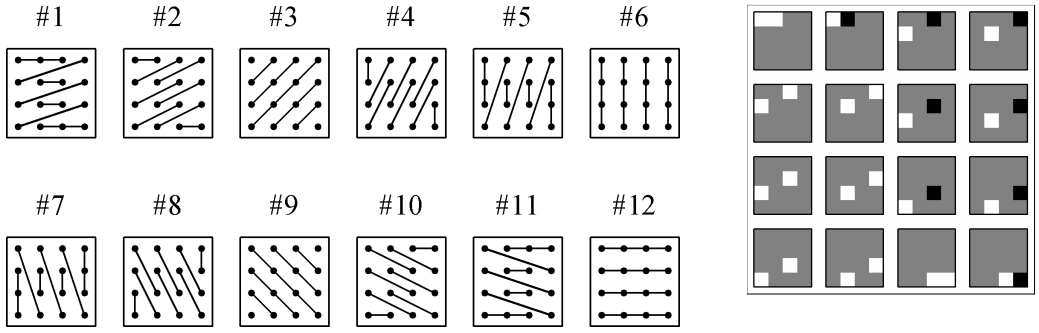

(a) (b)

Fig. 5. (a) The 12 grouping configurations. (b) Basis vectors for direction #2.

4 Dictionaries of bases

This section studies the dictionary composition. The aim is to obtain a low complexity yet efficient post-transform.

4.1 Bandelet Transform by groupings

The bandelet bases In [15], Peyré has proposed the bandelet bases by groupings and described the post-transform framework. Directional bases are built by linking coefficients along the same direction as displayed on figure 5(a). Discrete Legendre polynomials up to a degree $n-1$ are assigned to the groupings of n coefficients to form orthonormal bases. The vectors $\phi_{b,m}, m = 1, ..., M$, of the directional basis #2 are displayed on figure 5(b). The DCT basis and two Haar bases with different levels of resolution are added to these bases to form the dictionary of bandelet bases. Those additional bases are intended to be selected on blocks where directional basis are ineffective like blocks of textures. Figure 6(b) presents the results of the bandelet analysis on the LH_1 subband of the image 6(a). The bases have been selected according to the rate-distortion criterion (2) and are depicted on each 4×4 blocks.

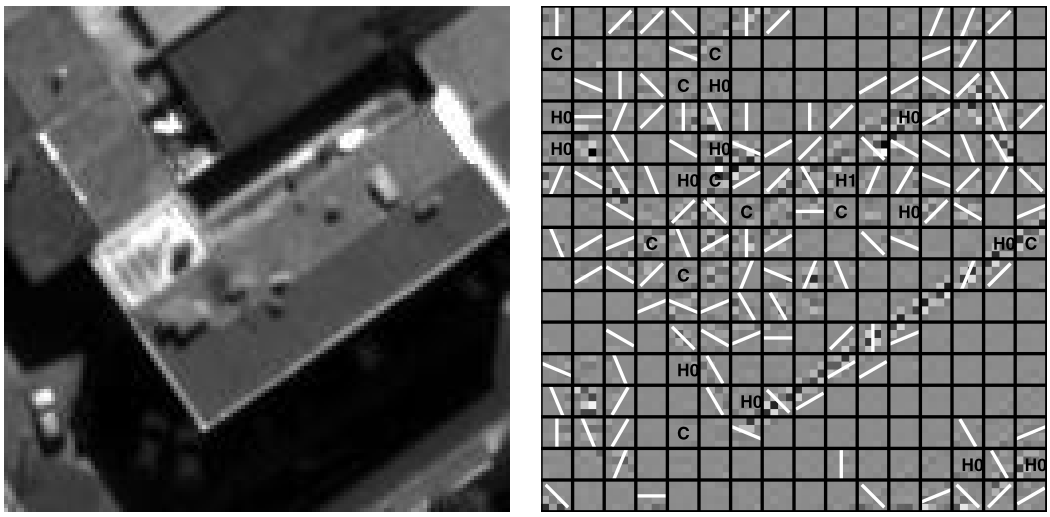

(a) Image (b) LH_1 subband

Fig. 6. PELICAN airborne sensor image (30 cm resolution) and the selected bandelet bases for LH_1 subband.

Blocks marked with a white line are post-transformed in a directional basis, blocks marked with H0 or H1 in a Haar basis and block marked with a C in the DCT basis. Other blocks are not post-transformed. The selected basis directions are rarely related to the edge directions for two main reasons. First, directions can hardly be distinguished on small blocks of 4×4 coefficients. Second, geometrical information is not considered in the best basis selection criterion (2).

Exploited mutual information The intra-block statistical redundancies exploited by the bandelet bases is analysed on the subbands HL_1, LH_1 and HH_1 of seven Earth observation images of size 1024×1024. Estimations are are performed on 7×16384 blocks for each subband HL_1, LH_1 and HH_1. The quantization step remains $q = 32$. Blocks of DWT coefficients are classified according to their best post-transform representation. DWT blocks that are best represented in the directional basis $\#b$ according to the rate-distortion cost

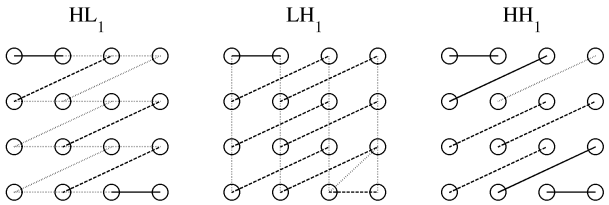

Fig. 7. Mutual information of pairs of wavelet coefficients from blocks of class #2.

(2) compose the b^{th} class. Figure 7 displays the relative mutual information in each pair of quantized DWT coefficients from blocks of the subbands HL_1, LH_1 and HH_1 that are best represented in the directional basis #2. This class contains 4335 blocks for the HL_1 subbands, 4340 blocks for the LH_1 subbands and 1909 blocks for the HH_1 subbands. The lines between two coefficients represent the relative mutual information I_r defined in equation (1). Plain lines are for $I_r \geq 20\%$, dashed lines are for $16\% \leq I_r < 20\%$ and dotted lines are for $10\% \leq I_r < 16\%$. Mutual information of DWT coefficients pairs fit the directional groupings of the bandelet basis #2. The dependency is thus well exploited by this basis in all the subbands. Nevertheless, it can be observed that dependency in the direction of the high-pass wavelet filter is not always exploited in the subbands HL_1 and LH_1.

Correlation analysis Similarly, figure 8 displays the correlation coefficients r for each pair of DWT coefficients from blocks in class #2. Plain lines are for $|r| \geq 0.5$, dashed lines are for $0.4 \leq |r| < 0.5$ and dotted lines are for $0.25 \leq |r| < 0.4$. Since few correlations appear in the direction of the groupings, it can be said that the directional basis #2 does not exploit much correlations. The correlations observed correspond to the direction of the high-pass wavelet filter. The same holds for the other block classes. Based on these observations, new bases that better decorrelate the DWT coefficients are built in

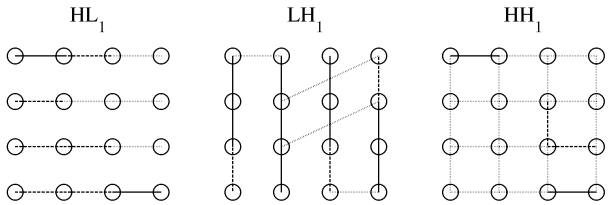

Fig. 8. Correlations in pairs of wavelet coefficients from blocks of class #2.

section 4.2. In particular, the statistical properties of each subband are taken into account.

4.2 Dictionary of bases derived from image statistical analysis

A better reduction of redundancies may be obtained from a dictionary derived from a statistical image analysis. A set of relevant images is processed off-line to build a so-called exogenic dictionary which will be used for the compression of any other images. The natural way to reduce correlations in a random process is to perform a Principal Component Analysis (PCA). This is consistent with the transform coding principles in which data are first decorrelated so as to reduce the zero order entropy [2]. One key point to improve the compression performance is to build one dictionary per subband. In this way, neither the complexity nor the side information are increased.

Bases built by PCA on each subband One PCA has been performed on each subband of the DWT of a learning set of images. The resulting bases are displayed on figure 9. The vectors are sorted column-wise by decreasing eigen values. Note that the vectors of principal component exhibit the low-pass and high-pass directions of the wavelet filters. For compression, blocks of DWT coefficients can either be post-transformed in the adapted PCA basis

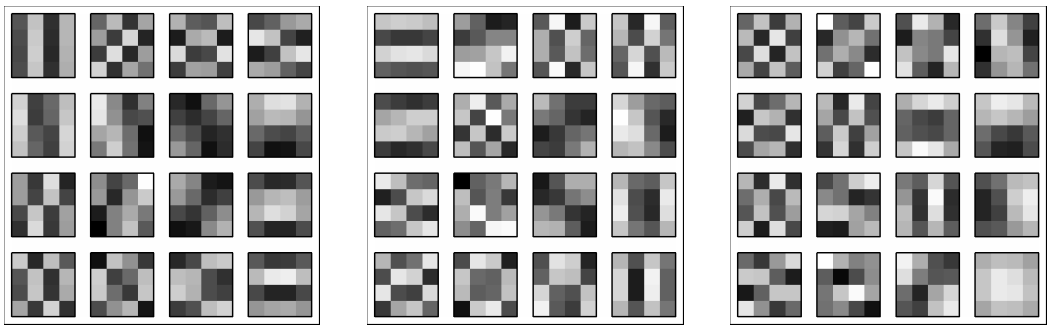

(a) PCA basis on HL_1 (b) PCA basis on LH_1 (c) PCA basis on HH_1

Fig. 9. Bases built by PCA for each subband HL_1, LH_1 and HH_1.

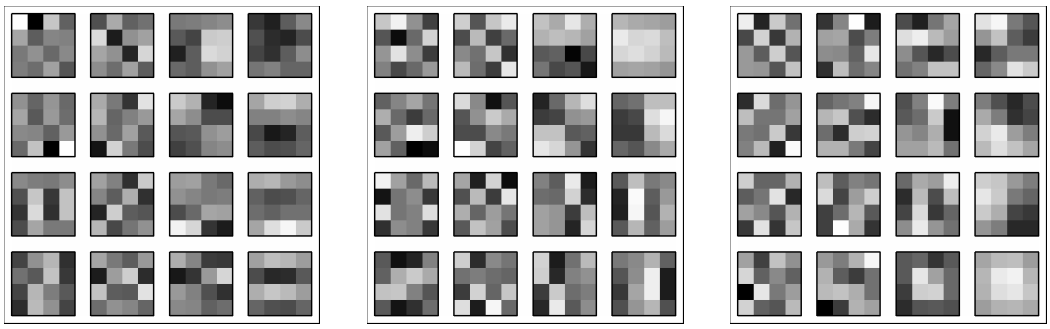

(a) HL_1 (b) LH_1 (c) HH_1

Fig. 10. Bases built by PCA on the block classes #2 for each subband.

or not post-transformed. The computational cost is limited since only one post-transform is computed. One key advantage of the PCA bases over the bandelet bases is that vectors are sorted in decreasing energy order. Thus, high magnitude coefficients are expected on the first vectors of those bases. An entropy coder could exploit this prior knowledge.

Bases built by PCA on each class of blocks For a fair comparison between PCA and the directional bandelets with respect to the number of bases, we have built 12 PCA bases adapted to the 12 classes of blocks built in section 4.1 [25]. The PCA bases built on class #2 in the subbands HL_1, LH_1 and HH_1 are displayed on figure 10. The goal is to remove the correlations

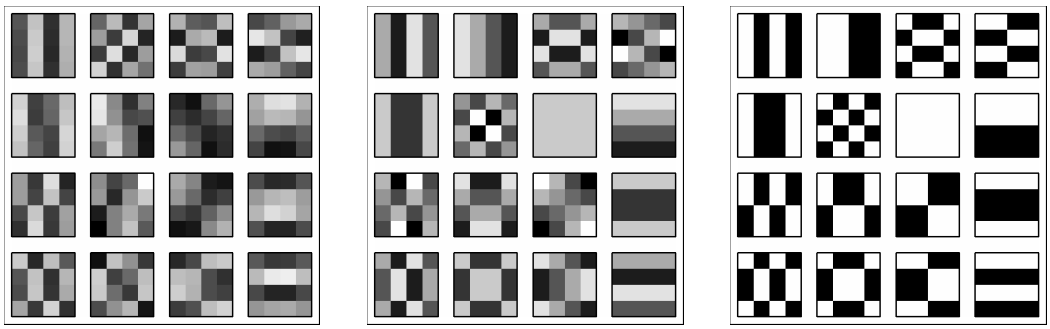

(a) PCA basis on HL_1 (b) DCT basis (c) Hadamard basis

Fig. 11. Basis vectors by decreasing energy order for HL_1 subband.

observed in those classes on figure 8. These new PCA bases are successful in this task. The maximum correlations observed on a set of six test images, outside the learning set, are less than 0.2 in these PCA bases although they are more than 0.5 in the directional bandelet bases. Other dictionaries of bases may be created based on other criteria to form the different classes of blocks. For example, specialized bases may be built for seas, forests, fields or city areas.

4.3 Standard bases

As shown on figure 11, when the vectors have been reorganized, the DCT basis and the PCA basis are similar. Thus, the DCT can be used as a post-transform with the main advantage that it can be computed using well-known fast algorithms. The same holds for the even simpler Hadamard transform involving only sums and differences of the DWT coefficients without multiplication. The required normalization by 4 can be done by 2 bit shifts. Figure 12 shows the approximation rate of HL_1 wavelet coefficients for the post-transform in the PCA, DCT and Hadamard bases. $\hat{f}_M$ denotes the approximation of the block of DWT coefficients f from the M largest post-transformed coefficients. The

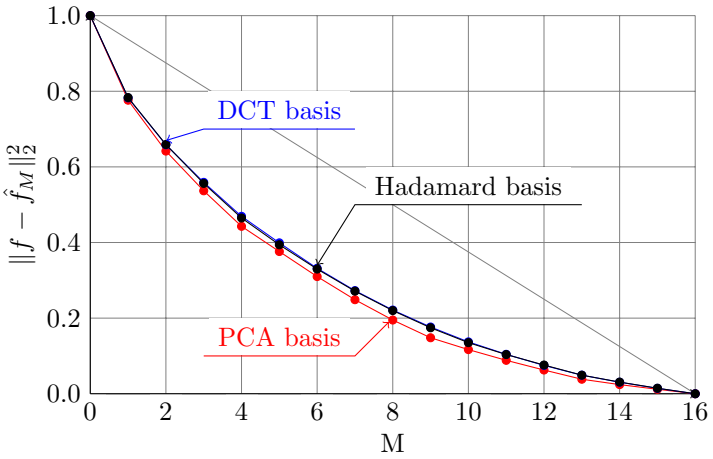

Fig. 12. Approximation rates of HL_1 wavelets coefficients.

approximation rate is similar in the three bases. The advantage of the PCA is thus limited since the other bases require less computational complexity.

5 Compression results

5.1 Post-transform with a multiple bases dictionary

If the computational power is sufficient to allow a large dictionary, PCA is a possible solution to build multiple bases. One basis may be built for each relevant class of blocks as described in section 4.2. Figure 13 presents the mean compression results obtained on a set of six 1024×1024 Earth observation images from PLEIADES satellite and PELICAN airborne sensor. The PELICAN sensor provides images with the spatial resolution expected for future satellite images. These images are 12-bits depth. This figure compares the compression performance obtained with the 12 directional bandelet bases, the 15 bandelet bases (including the DCT and the two Haar basis) and the 12 bases built by PCA. According to figure 13, the PSNR with the 12 PCA bases is around 0.2 dB greater than the PSNR with the 12 directional bandelet

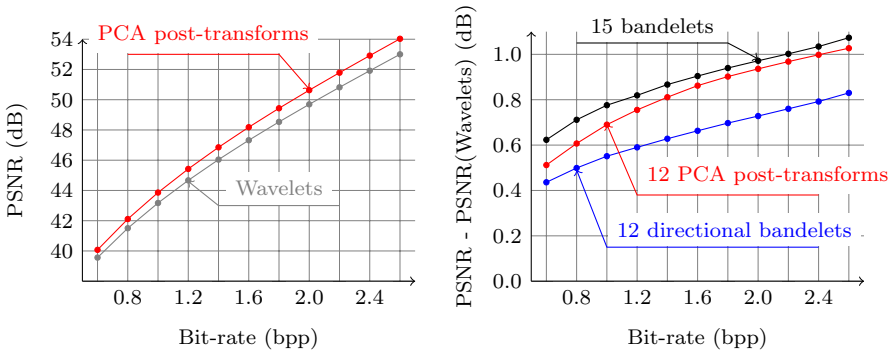

Fig. 13. Gain of PSNR with respect to the wavelet transform of the post-transform with the 12 PCA bases, the 12 directional bandelet bases and the 15 bandelet bases.

bases and is close to the PSNR with the 15 bandelet bases. Yet it has been observed that the addition of the DCT and two Haar bases to the 12 PCA dictionary does not significantly increase the performance. In this case, at 2 bpp the PSNR is 50.649 dB while it is 50.667 dB with the 15 bandelet bases. At other rates, PSNR are always slightly lower than those obtained with 15 bandelet bases. Indeed, the PCA are more similar to the DCT basis than the directional bandelet bases. Consequently, the DCT basis is more efficient and more often selected when used in conjunction with the directional bandelet bases. Another way to enlarge the PCA dictionary is to define more blocks classes and thus more PCA bases. However, the complexity increases almost linearly with the number of bases contrarily to the compression performance: the 12 PCA post-transform is far from being 12 times more efficient than a one PCA post-transform. In terms of compression performance, 15 bandelet bases seems a better choice than the 12 or even 15 PCA bases when the dictionary size is not limited by the complexity. Moreover, note that 70% of the bandelet coefficients are equal to zero. Hence, a smart implementation may lead to a smaller computational complexity with the 15 bandelet bases than with the 12 PCA bases, regarding the projection on the basis elements. This advantage

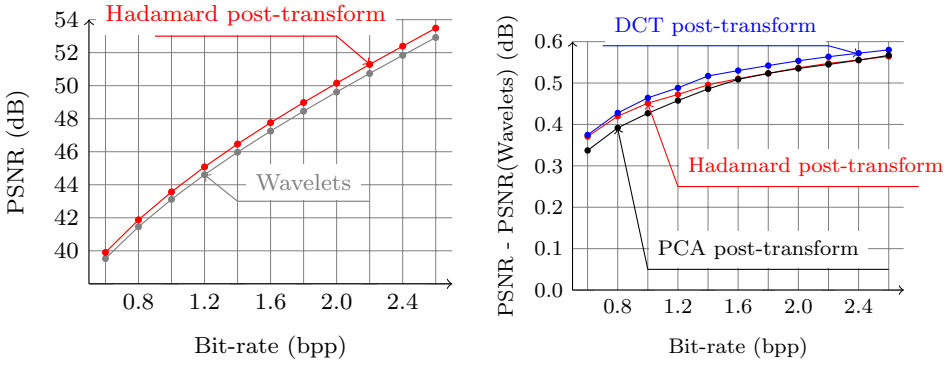

(a) (b)

Fig. 14. PSNR (a) and gain of PSNR with respect to the DWT (b) using a one basis dictionary.

must be balanced by the increased complexity of the rate-distortion criterion derivation for the 15 bases with respect to 12 bases regarding the rate estimation. Nevertheless, if sufficient computational power is available, the bandelet transform with 15 bases is a good choice.

5.2 Post-transforms using one basis

However, on-board satellites, the computational power may allow only a one basis post-transform. Figure 14 displays the compression performance obtained in this case. Figure 14(a) compares compression results obtained with the Hadamard post-transform and the DWT coefficients without post-transform. Figure 14(b) compares the performance of the different post-transform dictionaries, i.e. the PCA bases (one per subband), or the DCT basis, or the Hadamard basis relatively to the compression results of the DWT coefficients. Obviously, the post-transform using a dictionary consisting of only one basis improves the compression performance. For an approximate target rate of 2 bpp, a typical bit-rate in on-board applications, the PSNR increase is between 0.4 dB and 0.6 dB compared to the DWT alone. The results obtained

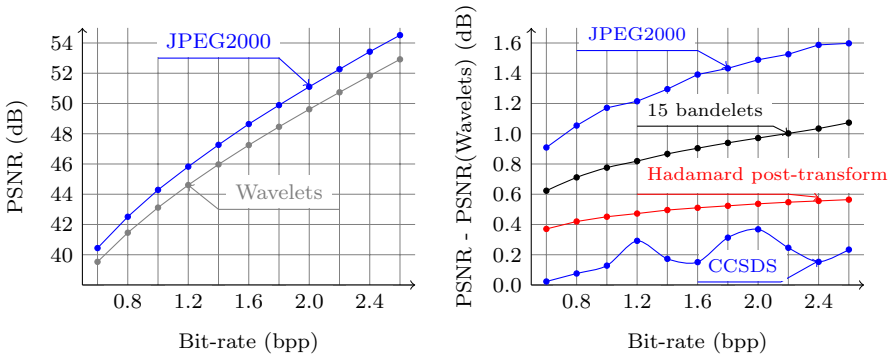

Fig. 15. Hadamard post-transform and bandelet transform compared to JPEG2000 and the CCSDS coder on six Earth observation images.

with the PCA, the DCT and the Hadamard bases are similar. When complexity constraints impose a one basis post-transform, the use of a PCA basis on each subband is not recommended unless the learning set is sufficiently representative. The DCT post-transform is less complex and gives good results. Yet, Hadamard basis could be advised since it is even less complex with similar compression performance. Moreover, the energy compaction property of the Hadamard basis, emphasized on figure 12, could also be exploited by the entropy coder.

5.3 Comparison to the standards

Figure 15 compares the performance of the post-transform with the Hadamard basis and bandelet transform with 15 bases to the CCSDS and JPEG2000 coder at bit-rates close to the targeted bit-rate of 2.0 bpp. In the CCSDS coder, the BPE uses tables of variable length codes for a very low complexity entropy coding. On the contrary in JPEG2000, EBCOT uses the contextual adaptive arithmetic coder called MQ-coder [9] with a rate-distortion optimization process to sort the "code-blocks" in the best order. There exists no such

optimization process in the BPE. Although a context modeling could take advantage of particular statistical distribution of the post-transform coefficients, in the proposed work, an adaptive arithmetic coder without context is applied directly on the post-transform coefficients.

The compression performance obtained with the bandelet transforms in 15 bases are still 0.5 dB under the results obtained with JPEG2000. However, even the less complex Hadamard post-transform outperforms the CCSDS coder. Moreover, as post-transforms applied on small blocks, they are suitable for the scan-based mode. Note that the performance in figure 15 are obtained in scan-based mode for the CCSDS but in frame-based mode for JPEG2000. Although JPEG2000 includes a scan-based mode compatible with strip compression, this feature is not provided in available softwares such as OpenJPEG or Kakadu. According to [16,26], the scan-based JPEG2000 performance is approximately reduced by 0.5 dB at 2.0 bpp compared to the frame-based mode, due to additional headers in each strip. In [27], a full low complexity compression scheme using the post-transform in Hadamard basis and the BPE coder has been proposed. This compression scheme even reduces the computational complexity of the best basis selection. The Lagrangian rate-distortion criterion is replaced by a l_1 norm minimization: a sum of the post-transform coefficients replaces the rate and distortion estimations. This compression scheme has a complexity sufficiently small to be implemented on-board satellite. Moreover the results obtained are 0.17 dB better than those of the CCSDS. Table 5 sums up the performance of the compression schemes mentioned. Reference compression times [2] have been obtained on a linux PC with an Intel CPU at

[2] Ref. 1 has been obtained with the the QccPack [20], ref. 2 with an implementation of the CCSDS 122 coder [1] from NASA and ref. 3 with Kakadu software.

Coder	Rate control	Transform	On-board compliance	Relative complexity	PSNR gain at 2.0 bpp
Adaptive arithmetic coder	Impossible	DWT	No	ref. 1 = 0.52 μs/sample	0 dB (reference)
		15 bandelets ($N_{\mathcal{B}} = 15$)	No	ref. 1 + $(N_{\mathcal{B}} \times 2M^2)/M$	+0.97 dB
		Hadamard PT	No	ref. 1 + $(M \log_2 M)/M$	+0.54 dB
BPE	Full and easy	DWT (CCSDS)	Yes	ref. 2 = 0.36 μs/sample	+0.37 dB
		Hadamard PT	Yes	ref. 2 + $(M \log_2 M)/M$	+0.54 dB [27]
EBCOT (JPEG2000)	Limited and complex	Scan-based	Not in hardware		$\approx$+1 dB [16,26]
		Frame-based	No	ref. 3 = 0.56 μs/sample	+1.49 dB

Table 5

Performance summary of different compression schemes.

1.86 GHz and 1 Go memory for the compression of a simulated PLEIADES image of size 2048×2048 at 2 bpp. From simulations, JPEG2000 frame-based results at 2.0 bpp are better than those of the CCSDS by 1.1 dB. Thus according to [16,26], JPEG2000 scan-based results may be around 0.6 dB better than those of the CCSDS. Thus, with a post-transform compression scheme having a low complexity, the results obtained may be only around 0.5 dB lower than those of JPEG2000 in scan-based mode.

6 Conclusion

This article has presented a new coding scheme based on post-transforms in the wavelet domain and inspired from the bandelet theory. The remaining linear dependencies between wavelet coefficients have been analyzed. The post-transform compression scheme has been designed to efficiently reduce these remaining correlations. This paper shows also that, in the case of satellite images, the bandelet directional bases are hardly related to the image geometric features. The redundancy actually exploited in the grouping direction can be measured by the mutual information but some correlations found between

neighboring wavelet coefficients are not exploited. This type of redundancy is better exploited by the use of PCA bases. The post-transform process requires the decomposition on all the dictionary bases for rate-distortion optimization. If enough computational power is available, the choice of the dictionary of 15 bandelet bases is advised rather than the dictionary of PCA bases. Using an arithmetic coder, the average gain over the wavelet transform would reach 1.0 dB at the targeted rate of 2.0 bpp. In the case of on-board satellite compression, the low complexity yet efficient Hadamard basis would generally be advised. The average gain at 2.0 bpp would then be 0.5 dB in PSNR. The post-transform process can be adapted to make it suitable to an embedded bit-plane coder such as the BPE of the CCSDS recommendation, resulting in a sufficiently low-complexity coder for on-board compression. Note that the average gain obtained with the post-transform scheme results from a local distortion decrease near the edges. Usual image post-processing such as segmentation should take advantage of this property.

7 Acknowledgments

This work has been carried out under the financial support of the French space agency CNES (www.cnes.fr) and NOVELTIS company (www.noveltis.fr). We also thank G. Peyré for the useful discussions and for the software components provided.

References

[1] CCSDS, *Image Data Compression Recommended Standard CCSDS 122.0-B-1 Blue Book*, Nov. 2005.

[2] V. K. Goyal, "Theoretical foundations of transform coding," *IEEE Signal Processing Mag.*, pp. 9–21, Sept. 2001.

[3] J. Liu and P. Moulin, "Information-theoretic analysis of interscale and intrascale dependencies between image wavelet coefficients," *IEEE Trans. on Image Processing*, vol. 10, pp. 1647 – 1658, Nov. 2001.

[4] R. W. Buccigrossi and E. P. Simoncelli, "Image compression via joint statistical characterization in the wavelet domain," *IEEE Trans. on Image Processing*, vol. 8, pp. 1688–1701, Dec. 1999.

[5] Z. Azimifar, *Image Models for Wavelet Domain Statistics*. PhD thesis, University of Waterloo, Ontario, Canada, 2005.

[6] J. M. Shapiro, "Embedded image coding using zerotrees of wavelet coefficients," *IEEE Trans. on Signal Processing*, vol. 41, no. 12, pp. 3445–3462, 1993.

[7] A. Said and W. A. Pearlman, "A new fast and efficient image codec based on set partitioning in hierarchical trees," *IEEE Trans. on Circuits and Systems for Video Technology*, vol. 6, pp. 243–250, 1996.

[8] ISO/IEC JTC 1/SC 29/WG 1, *JPEG 2000 Part I Final Committee Draft Version 1.0*. JPEG 2000 Editor Martin Boliek, Mar. 2000.

[9] D. Taubman and M. Marcellin, *JPEG2000: Image compression fundamentals, standards and practice*. Kluwer Academic Publishers, 2001.

[10] S. D. Servetto, K. Ramchandran, and M. T. Orchard, "Image coding based on a morphological representation of wavelet data," *IEEE Trans. on Image Processing*, vol. 8, pp. 1161–1174, Sept. 1999.

[11] F. Lazzaroni, R. Leonardi, and A. Signoroni, "High-performance embedded morphological wavelet coding," *IEEE Signal Processing Letters*, vol. 10, pp. 293–295, Oct. 2003.

[12] E. J. Candes and D. L. Donoho, "Curvelets - a surprisingly effective nonadaptive representation for objects with edges," in *Curves and Surfaces* (L. S. et al., ed.), Nashville, TN, Vanderbilt University Press, 1999.

[13] M. N. Do and M. Vetterli, "The contourlet transform: an efficient directional multiresolution image representation," *IEEE Trans. on Image Processing*, vol. 14, pp. 2091–2106, Dec. 2005.

[14] G. Peyré and S. Mallat, "Discrete bandelets with geometric orthogonal filters," in *Proc. of ICIP'05*, vol. 1, pp. 65–68, Sept. 2005.

[15] G. Peyré, *Géométrie multi-échelle pour les images et les textures*. PhD thesis, École Polytechnique, 2005.

[16] CCSDS, *Image Data Compression Informational Report CCSDS 120.1-G-1 Green Book*, June 2007.

[17] X. Delaunay, M. Chabert, G. Morin and V. Charvillat, "Bit-plane analysis and contexts combining of JPEG2000 contexts for on-board satellite image compression," in *Proc. of ICASSP'07*, pp. 1057–1060, IEEE, Apr. 2007.

[18] P. Lier, G. Moury, C. Latry, and F. Cabot, "Selection of the SPOT-5 image compression algorithm," in *Earth Observing Systems III* (W. L. Barnes, ed.), vol. 3439-70, pp. 541–552, San Diego, CA, SPIE, Oct. 1998.

[19] A. Robert, I. Amonou, and B. Pesquet-Popescu, "Improving DCT-based coders through block oriented transforms," in *Advanced Concepts for Intelligent Vision Systems* (S. B. . Heidelberg, ed.), vol. 4179, pp. 375–383, LNCS, 2006.

[20] J. E. Fowler, "QccPack: An open-source software library for quantization,

compression, and coding," in *Applications of Digital Image Processing XXIII* (A. G. Tescher, ed.), San Diego, CA, pp. 294–301, SPIE, Aug. 2000.

[21] F. Falzon and S. Mallat, "Analysis of low bit image transform coding," *IEEE Trans. on Signal Processing*, vol. 46, pp. 1027–1042, Apr. 1998.

[22] E. Le Pennec and S. Mallat, "Sparse geometric image representations with bandelets," *IEEE Trans. Image Processing*, vol. 14, pp. 423–438, Apr. 2005.

[23] X. Delaunay, E. Christophe, C. Thiebaut, and V. Charvillat, "Best post-transform selection in a rate-distortion sense," in *Proc. of ICIP'08*, Oct. 2008.

[24] Y. Shoham and A. Gersho, "Efficient bit allocation for an arbitrary set of quantizers," *IEEE Trans. on Acoustics, Speech, and Signal Processing*, vol. 36, pp. 1445–1453, Sept. 1988.

[25] X. Delaunay, M. Chabert, V. Charvillat, G. Morin, and R. Ruiloba, "Satellite image compression by directional decorrelation of wavelet coefficients," in *Proc. of ICASSP'08*, pp. 1193–1196, IEEE, Apr. 2008.

[26] J. C. Rountreea, B. N. Webba, M. W. Marcellin, "Testing JPEG 2000 Compression for Earth Science Data," in *Proc. NASA Earth Science Technology Conf.*, 2002.

[27] X. Delaunay, C. Thiebaut, E. Christophe, R. Ruiloba, M. Chabert, V. Charvillat and G. Morin, "Lossy compression by post-transforms in the wavelet domain," in *On-Board Payload Data Compression Workshop*, June 2008.